Focusing properties of near-field time reversal

Julien de Rosny and Mathias Fink
Laboratoire Ondes et Acoustique, CNRS/ESPCI/Université Paris VII, UMR 7587, 10 rue Vauquelin, 75005 Paris, France
(Received 11 September 2007; published 6 December 2007)

A time-reversal mirror (TRM) is a plane apparatus that generates the time symmetric of a wave produced by an initial source. Here we look for the conditions to obtain subwavelength focusing when the initial source is in the near field of the TRM and the propagating medium is homogeneous and isotropic. Three variants of TRM are studied: TRM made of monopoles, dipoles, or both of them. The analysis is performed in terms of evanescent and propagative waves. We conclude that only the dipole-TRM leads to subwavelength focusing.

DOI: 10.1103/PhysRevA.76.065801 PACS number(s): 42.25.Fx, 03.50.−z, 02.30.Nw, 43.20.+g

I. INTRODUCTION

In classical wave imaging, the resolution of any apparatus (optical, acoustical, etc.) cannot be better than half the wavelength. This limitation is due to the fact that subwavelength details are carried by evanescent waves, which decrease exponentially with the propagation distance and usually do not reach the imaging system. As a consequence, the subwavelength details are lost.

To overcome this limitation, near-field spectroscopy techniques have been developed for surface imaging [1]. Basically, a single subwavelength scatterer, which is very close to the surface, locally converts the evanescent waves into propagative ones. Scanning this scatterer across the surface allows a far-field reconstruction of the near-field image. More recently, the concept of superlens has been proposed for subwavelength imaging [2]. These superlenses are made of a slab of left-handed material [3]. In such a material both the permittivity and the permeability are negative, the index of refraction equals −1, and the evanescent components are exponentially amplified within the slab's thickness [4].

Time reversal has been proposed to focus a wave field below the half wavelength limit. The time-reversal technique is well known in acoustics and has led to a number of applications [5]. A focal spot as small as one-thirtieth of a wavelength has been reported when a time-reversal mirror (TRM) backpropagates a wave inside a microstructured medium. In such a medium, the propagative waves are converted back into evanescent components [6] and subwavelength focusing is achieved. As the resolution is due to the microstructured medium, the TRM can be in the far field of the initial source without losing the subwavelength focusing.

Contrary to microstructured media, the TRM has to be in the near field of the initial source in a homogeneous medium in order to get subwavelength focusing. Recently, experimental results in such a configuration have been reported in acoustics [7]. Here we propose a systematic approach of near-field time-reversal focusing in homogeneous media. We introduce three species of TRM: The perfect one, the dipole one, and the monopole one. In each case, to obtain the focusing property of the TRM, we explicitly write the two-dimensional Fourier transform of the time-reversed field. The results of this study are rather surprising: A perfect TRM will never focus a wave on a subwavelength spot size even if the TRM is infinitely close from the initial source. We show that a subwavelength focal spot can only be obtained with the dipole TRM.

II. TIME-REVERSAL BASICS

Let us introduce a Cartesian coordinate system $Oxyz$. During the first step of the time-reversal operation, a distribution of sources included in the plane Oxy emits a wave. For simplicity, we deal with monochromatic sources of complex amplitude. The time dependent expressions can be deduced by an inverse Fourier transform. The phase and the amplitude of the wave field (ϕ) and its first normal derivative ($\partial_n \phi$) are measured on each point of two infinite planes. These two planes are parallel to the x,y plane at the distance d in the positive and negative z directions, respectively. During the second step of time reversal, these signals are flipped in time, i.e., phase conjugated at each frequency and then reemitted from these planes. It has been shown [8] that the time-reversal principle is based on the Green's theorem. Consequently a perfect TRM contains both monopole and dipole sources. The axis of the dipoles are perpendicular to the TRM plane. The monopole sources emit the phase conjugated normal derivative signals and the dipole sources emit the phase conjugated signals. The analytical expression of the field $\phi_{\mathrm{TR/P}}$ created by two such perfect TRM is

$$\phi_{\mathrm{TR/P}}(x,y,z) = \sum_{z_0=-d,+d} \int [G(x-x_0,y-y_0,z-z_0) \times \partial_n \phi^*(x_0,y_0,z_0) - \phi^*(x_0,y_0,z_0)\partial_n G(x-x_0,y-y_0,z-z_0)]dx_0 dy_0, \quad (1)$$

where G is the Green's function. A two-dimensional Fourier transform over x and y variables yields

$$\phi_{\mathrm{TR/P}}(k_x,k_y,z) = \sum_{z_0=-d,+d} G(k_x,k_y,z-z_0)\partial_n \phi^*(k_x,k_y,z_0) - \phi^*(k_x,k_y,z_0)\partial_n G(k_x,k_y,z-z_0). \quad (2)$$

From a practical point of view, it is very difficult to perform such an ideal time reversal. Usually, the same device is used as an emitter and a receiver (e.g., acoustic transducers, electromagnetic antennas, etc.). Moreover, most of the time, these transceivers are reciprocal. That means, for instance, when the emitting pattern of a monopole transceiver is omnidirectional, the receiving one is also omnidirectional. This property also stands for dipole transceivers. Consequently, the two-dimensional Fourier transform of the field $\phi_{TR/M}$ generated by a TRM that is only made of monopole transceivers is given by

$$\phi_{TR/M}(k_x,k_y,z) = \sum_{z_0=-d,+d} G(k_x,k_y,z-z_0)\phi^*(k_x,k_y,z_0). \quad (3)$$

As for a TRM only made of dipole transceivers, the Fourier transform of the field $\phi_{TR/D}$ leads to

$$\phi_{TR/D}(k_x,k_y,z) = \sum_{z_0=-d,+d} \partial_n G(k_x,k_y,z-z_0)\partial_n\phi^*(k_x,k_y,z_0). \quad (4)$$

Note that the subscripts "TR/P," "TR/M," and "TR/D" stand for perfect, monopolar, and dipolar time reversal, respectively.

III. POINTLIKE INITIAL SOURCE

From now on, we assume that the initial source is pointlike at position O. In other words, the source distribution equals $-\delta(x,y,z)$. As a result, the field ϕ is equal to the Green's function. In order to calculate Eqs. (2)–(4), we first work out the analytical expression of the two-dimensional Fourier transform of the Green's function. The Green's function is the solution of the Helmoltz equation with a source term,

$$(\nabla^2+\omega^2-i\omega\varepsilon)G(x,y,z) = -\delta(x,y,z). \quad (5)$$

Because we only deal with homogeneous propagation media, the wave speed is set to 1 without loss of generality. A weak attenuation in the propagation medium is considered by adding the term $-i\varepsilon\omega$. The attenuation coefficient ϵ will be larger than zero only when the case of the monopole TRM will be considered. Indeed, we shall see that this attenuation coefficient is needed in order to regularize the mathematical expression of the time-reversed field. The expression of the two-dimensional Fourier transform over (x,y) coordinates of G is given by

$$G(k_\parallel,z) = \frac{1}{2}\frac{\exp(-\sqrt{k_\parallel^2-\omega^2+i\omega\epsilon}|z|)}{\sqrt{k_\parallel^2-\omega^2+i\omega\epsilon}}, \quad (6)$$

where $k_\parallel=\sqrt{k_x^2+k_y^2}$. Introducing $\alpha_\perp$ such that $\alpha_\perp=\sqrt{k_\parallel^2-\omega^2+i\omega\epsilon}$, the expressions of the fields given by Eqs. (2)–(4) become

$$\phi_{TR/P}(k_x,k_y,z) = \frac{\mathrm{Im}\alpha_\perp}{|\alpha_\perp|^2}\exp(-2d\,\mathrm{Re}\alpha_\perp)\cosh(\alpha_\perp z), \quad (7)$$

$$\phi_{TR/M}(k_x,k_y,z) = +\exp(-2d\,\mathrm{Re}\alpha_\perp)\frac{\cosh(\alpha_\perp z)}{2|\alpha_\perp|^2}, \quad (8)$$

$$\phi_{TR/D}(k_x,k_y,z) = -\exp(-2d\,\mathrm{Re}\alpha_\perp)\frac{\cosh(\alpha_\perp z)}{2}, \quad (9)$$

where Re and Im refer to the real and the imaginary parts of the argument, respectively. Similar expressions are worked out in [9] where the aim is to study the behavior of time-reversal mirrors mounted in soft or rigid planar baffle. But no attention is paid to the time-reversal properties when the point source is close to the time-reversal mirror.

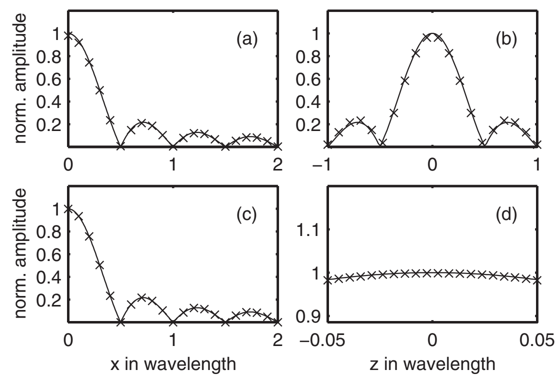

FIG. 1. Time-reversed fields along the z axis [(a) and (c)]and along the x axis [(b) and (d)]. The distance between the TRM equals two wavelengths (d=1) for subplots (a) and (b). The distance is 0.1 wavelength (d=0.05) for subplots (c) and (d). Here the time-reversal method is the perfect one (see text). The × marks are obtained by numerical integration of Eq. (10) and the continuous lines result from the analytical expression (14).

Finally, an inverse Fourier transform is performed that leads to the spatial dependence of the fields between the TR

$$\phi(x,y,z) = \frac{1}{2\pi}\int_0^\infty J_0(k_\parallel\sqrt{x^2+y^2})\phi(k_\parallel,z)k_\parallel dk_\parallel. \quad (10)$$

We have all the mathematical tools to study the time-reversed fields in terms of evanescent and propagating components for the three species of TRM.

A. Perfect time reversal

From Eq. (7), we deduce that $\phi_{TR/P}$ is equal to zero for the evanescent components because α is real when $k_\parallel>\omega$. As a consequence, the perfect time-reversal mirror cannot generate subwavelength details even when it is infinitely close to the original source point. This is confirmed in Fig. 1 where the field created by a perfect TRM is plotted. Introducing the normal wave vector $k_\perp$ ($\alpha_\perp=ik_\perp$), the expression of $\phi_{TR/P}$ when $k_\parallel<\omega$ becomes

$$\phi_{TR/P}(k_x,k_y,z) = i\frac{\cos(zk_\perp)}{k_\perp} \quad (11)$$

This last expression can be written in terms of the imaginary part of the two-dimensional Fourier transform of the Green's function,

$$\phi_{TR/P}(k_x,k_y,z) = -2i\,\mathrm{Im}G(k_x,k_y,z). \quad (12)$$

Doing a two-dimensional inverse Fourier transform, it readily becomes

$$\phi_{TR/P}(x,y,z) = -2i\,\mathrm{Im}G(x,y,z). \quad (13)$$

Here we find a fundamental property that came up with the first developments of the time-reversal theory [8] when the

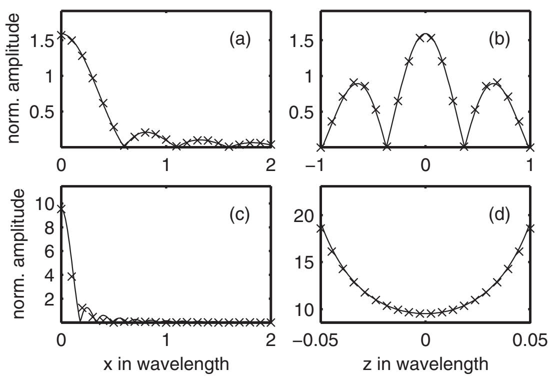

FIG. 2. Normalized time-reversed fields on the z axis (see Fig. 1 for details on the subplots). Here dipole transceivers time reverse the field. The $\times$ marks are obtained by numerical integration of Eq. (10) and the continuous lines result from Eqs. (15) and (16).

field and its normal derivative are time reversed from a closed surface. In our case, the two TR planes do not form a closed surface but as the field vanishes at large distance and the TR planes are boundless, it is natural to find Cassereau and Fink's result.

In a homogeneous medium, the Green's function is given by $G(x,y,z)=e^{-i\omega R}/4\pi R$, where $R=\sqrt{x^2+y^2+z^2}$. Consequently, the time-reversed field is given by

$$\phi_{\mathrm{TR/P}}(x,y,z) = i\frac{\sin(\omega R)}{2\pi R}. \tag{14}$$

Note that the focal spot size always equals half a wavelength regardless of the distance between TR planes (and more generally of the geometry of the close surface).

B. Dipole time-reversal mirrors

We now perform an imperfect time reversal where we assume that the TRM is only made of dipole transceivers (see Fig. 2). In such a case, Eq. (9) shows that $\phi_{\mathrm{TR/D}}$ is different from zero for evanescent components ($k_\parallel > \omega$). From Eqs. (9) and (10), the analytic expression of the field along the z axis is calculated,

$$\phi_{\mathrm{TR/D}}(0,0,z) = \frac{[\cos(\omega z) + \omega z\,\sin(\omega z) - 1]}{4\pi z^2} + \frac{(z^2+4d^2)}{4\pi(z-2d)^2(z+2d)^2}. \tag{15}$$

As for the field ψ in the plane Oxy, only an approximate expression can be derived,

$$\phi_{\mathrm{TR/D}}(x,y,0) \approx \left(\omega^2 + \frac{1}{2d^2}\right)\frac{J_1(k_m R)}{4\pi R k_m}, \tag{16}$$

where $k_m^2=\omega^2+1/d^2$. To obtain this expression, we approximate $\exp(-2d\,\mathrm{Re}\alpha_\perp)$ in Eq. (10) by a step function which equals 1 when $d\,\mathrm{Re}\alpha_\perp<1$ and 0 otherwise. This approximation gives rise to ripples in Fig. 1(c) because of the sharp integral cutoff.

When $d \gg 1/\omega$, which means that the TRM is in the far field of the source, the amplitude at the focus is given by $\omega^2/8\pi$ and the spatial dependence of the focal spot in plane Oxy is given by $J_1(\omega R)/2\omega R$. These two quantities are independent of the distance d, and the focusing is again diffraction limited. In the near-field limit ($d \ll 1/\omega$), $k_m \approx 1/d$ and the width of the focal spot in plane Oxy is roughly equal to $2d$, i.e., the distance between the two time-reversal mirror planes [see Fig. 2(c)]. Moreover, the amplitude of the focus is dominated by the evanescent components of the wave and is equal to $1/16\pi d^2$. Actually, the subwavelength focusing is due to the directivity of the dipole transceivers. Indeed, due to this directivity, the amplitude of the signal is higher when the transceivers that are just in front of the source. Due to transceiver reciprocity, the same effect occurs during emission of the phase conjugated field. This "geometrical" effect explains the lateral subwavelength focusing.

In the next section, we show that a nonperfect TRM does not necessarily imply subwavelength resolution.

C. Monopole time reversal

At first, looking at Eq. (8), we may think that the same subwavelength focusing effect occurs for TRM containing only monopoles. Indeed, the Fourier transform of $\phi_{\mathrm{TR/M}}$ contains evanescent components. However, we shall see that the focal spot size equals approximately half a wavelength in this case.

At position O ($x=y=z=0$) and without considering dissipation ($\alpha=0$), the integration in Eq. (7) goes to infinity because of the singularity at $k_\perp=\omega/c$. The physical meaning of this divergence is the following: The monopole sources generate waves that decrease as the inverse of the distance. So a monopole transceiver will produce at O a time-reversed field which is inversely proportional to the square of the distance between the transceiver's position and O. Introducing R as the distance between the transceiver and the z axis, the total time-reversed field amplitude is proportional to $2\pi\int R\,dR/(R^2+d^2)$. This integral diverges when the integration is performed between $R=0$ and $R=\infty$ because the integrand behaves for large distances as $1/R$, giving a logarithmic singularity. Actually, one can show that the TR field diverges not only at O but everywhere between the two TRM. This divergence is due to the fact that the contribution of monopoles included in an elementary ring with radius R and thickness dR does not vanish as R increases. To "regularize" the integral, we introduce a weak dissipation into the propagation equation ($\varepsilon>0$). The far contributions are therefore attenuated faster than $1/R$ and the TR field is finite. The upper integration domain is now limited to about $R=1/\sqrt{\omega\epsilon}$ because this distance is the attenuation length of the wave. The relative amount of TR field generated by monopoles farther than one wavelength from O is $1-2\pi\sqrt{\epsilon/\omega}$. If ϵ is small, the TR focal spot is mainly due to these far monopolar transceivers and it is therefore diffraction limited even when $d \ll \lambda$ (see Fig. 3).

To obtain an approximate analytical expression of the field on the z axis, first we assume that $d\sqrt{\omega\epsilon} \ll 1$, i.e., the attenuation length is much larger than the distance between

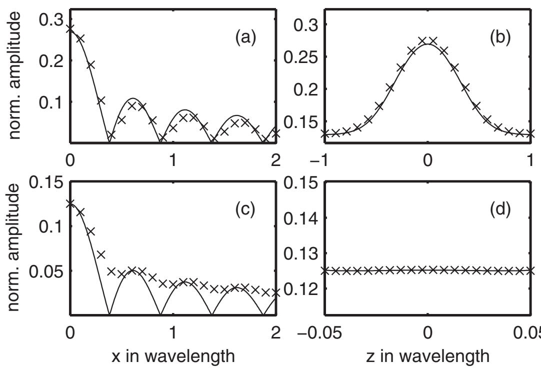

FIG. 3. Normalized time-reversed fields on the z axis (see Fig. 1 for details on the subplots). Here monopole transceivers time reverse the field. The $\times$ marks are obtained by numerical integration of Eq. (10) and the continuous lines result from Eqs. (17) and (18). The plots are obtained with an attenuation length $(1/\sqrt{\omega\epsilon})$ equal to a 126.2 wavelength.

the TRM. Second, we introduce an angular frequency Ω which is chosen such that $\sqrt{\omega\epsilon} \ll \Omega \ll 1/2d$ [11]. By dividing the integral domain of Eq. (10) into four intervals [12], we get for the time-reversed field on the z axis

$$\psi_{\mathrm{RT,M}}(0,0,z) \approx \frac{1}{8\pi}\{i\pi - Ci(\omega z) + Ci(\Omega z) + Ei(\Omega[z+2d]) + Ei(\Omega[2d-z])\}, \tag{17}$$

and the transverse focus pattern is given by

$$\psi_{\mathrm{RT,M}}(x,y,0) \approx \frac{J_0(\omega R)}{8\pi}\left[i\pi + 2\ln\left(\frac{\Omega}{\omega}\right) + 2Ei(2\Omega d)\right]. \tag{18}$$

To obtain this latter expression, it is, moreover, assumed that the main contribution for the spatial dependence of the field inside plane Oxy comes from the transverse components such that $k_{\parallel}=\omega$. In other words, we assume that the far transceivers only contribute to the focal spot, which is consistent with $d \ll 1/\sqrt{\omega\epsilon}$. In Fig. 3, we see that this approximation is particularly valid when the distance between the two TRM is small. Note that the angular frequency Ω has no physical meaning; it is a sort of "hidden" variable that has been introduced to obtain analytical expressions.

IV. CONCLUSION

As we have seen, near-field time reversal does not systematically imply subwavelength focusing. First, we have shown that a "perfect" TRM generates the imaginary part of the Green's function of a homogeneous medium. In such a medium, the imaginary part of the Green's function does not contain evanescent components. In other words, even when the TRM is very close to the focal spot, the time-reversal focusing is still diffraction limited. On the other hand, we have shown that when using monopole-only TRM or dipole-only TRM, the time-reversed field contains evanescent components. Nevertheless, subwavelength focusing is only achieved with a TRM made of dipole transceivers. Recently, a subwavelength focusing inside a strongly heterogeneous medium has been reported [10]. In such a case, the focus is still given by the imaginary part of the Green's function, but the near-field scattering of the wave off the medium's heterogeneities allows the Green's function to fluctuate faster than the wavelength.

[1] E. Betzig, J. K. Trauman, T. D. Harris, J. S. Weiner, and R. L. Ksotelak, Science **251**, 1468 (1991); F. Zenhausern, Y. Martin, and H. K. Wickramasinghe, *ibid.* **269**, 1083 (1995).
[2] J. B. Pendry, Phys. Rev. Lett. **85**, 3966 (2000); D. R. Smith, Science **308**, 502 (2005); J. B. Pendry and D. R. Smith, Sci. Am. **295**, 60 (2006).
[3] D. R. Smith, W. J. Padilla, D. C. Vier, S. C. Nemat-Nasser, and S. Schultz, Phys. Rev. Lett. **84**, 4184 (2000); R. A. Shelby, D. R. Smith, and S. Schultz, Science **292**, 77 (2001).
[4] V. G. Veselago, Sov. Phys. Usp. **10**, 509 (1968).
[5] M. Fink, Sci. Am. **281**, 91 (1999).
[6] R. Carminati, J. J. Sáenz, J.-J. Greffet, and M. Nieto-Vesperinas, Phys. Rev. A **62**, 012712 (2000).
[7] S. G. Conti, P. Roux, and W. A. Kuperman, J. Acoust. Soc. Am. **121**, 3602 (2007).
[8] D. Cassereau and M. Fink, IEEE Trans. Ultrason. Ferroelectr. Freq. Control **39**, 579 (1992).
[9] D. Cassereau and M. Fink, J. Acoust. Soc. Am. **94**, 2373 (1993).
[10] G. Lerosey, J. de Rosny, A. Tourin, and M. Fink, Science **315**, 1120 (2007).
[11] In practice, the geometric mean $(\Omega=\sqrt{\sqrt{\omega\epsilon}/2d})$ is used.
[12] The four intervals are $]0,\sqrt{\omega^2-\Omega^2}[$, $]\sqrt{\omega^2-\Omega^2},\omega[$, $]\omega,\sqrt{\omega^2+\Omega^2}[$, and $]\sqrt{\omega^2+\Omega^2},\infty[$. In such a case, $2\psi_{\mathrm{RT/M}}(0,0,z) \approx \int_0^{\Omega}[k'/(k'^2+i\omega\epsilon)]dk' + \int_{\Omega}^{\omega}[\cos(k'z)/k']dk' + \int_0^{\Omega}[\alpha'/(\alpha'^2+i\omega\epsilon)]d\alpha' + \int_{\Omega}^{\infty}[\cosh(\alpha'z)e^{-2\alpha'd}/\alpha']d\alpha'$.